# Plasma size and power scaling of ion temperature gradient driven turbulence

Yasuhiro Idomura, and Motoki Nakata

Citation: Physics of Plasmas **21**, 020706 (2014);
View online: https://doi.org/10.1063/1.4867379
View Table of Contents: http://aip.scitation.org/toc/php/21/2
Published by the American Institute of Physics

# Plasma size and power scaling of ion temperature gradient driven turbulence

Yasuhiro Idomura[1] and Motoki Nakata[2]
[1]*Japan Atomic Energy Agency, Kashiwanoha 5-1-5, Kashiwa, Chiba 277-8587, Japan*
[2]*Japan Atomic Energy Agency, Obuchi-Omotedate 2-166, Rokkasho, Kamikita, Aomori 039-3212, Japan*

(Received 15 November 2013; accepted 20 February 2014; published online 27 February 2014)

The transport scaling with respect to plasma size and heating power is studied for ion temperature gradient driven turbulence using a fixed-flux full-$f$ gyrokinetic Eulerian code. It is found that when heating power is scaled with plasma size, the ion heat diffusivity increases with plasma size in a local limit regime, where fixed-gradient $\delta f$ simulations predict a gyro-Bohm scaling. In the local limit regime, the transport scaling is strongly affected by the stiffness of ion temperature profiles, which is related to the power degradation of confinement. © *2014 AIP Publishing LLC*. [http://dx.doi.org/10.1063/1.4867379]

The plasma size scaling of turbulent heat transport is of critical importance in predicting performances of future fusion devices, which will be several times larger than the present experiments. Although this issue was addressed experimentally,[1,2] plasma size parameters of existing devices are far below reactor relevant regimes, and extrapolations of transport properties play critical roles in the reactor design studies.[3] On the other hand, with rapidly increasing computing power, the credibility of gyrokinetic simulations has dramatically improved,[4] and the plasma size scaling of turbulent transport has also been theoretically investigated based on numerical experiments with global gyrokinetic simulations.

In Ref. 5, the plasma size scaling of the ion temperature gradient driven (ITG) turbulence was first addressed using a $\delta f$ gyrokinetic particle code, and the transition of transport scaling from a Bohm like scaling to a gyro-Bohm like scaling was found for large devices. In Ref. 6, a key mechanism was proposed as spreading of turbulent fluctuations into linearly stable core and edge regions, which were prescribed in the simulation. In Ref. 7, the transition feature and saturation levels of the above transport scaling were quantitatively verified from comparisons of $\delta f$ gyrokinetic particle and Eulerian codes and of different MHD equilibrium models, and the transport scaling was explained by profile shearing, which is characterized by the effective plasma size or the size of high temperature gradient region.

Although several $\delta f$ gyrokinetic simulations give the converged transport scaling, it may not be experimentally relevant from the viewpoint of heating power. In plasma size scans with $\delta f$ gyrokinetic simulations, the plasma size $a/\rho_{ti} = \rho^{*-1}$ is varied with the fixed normalized temperature gradient, $R/L_{ti}$, where $a$ is the minor radius, $R$ is the major radius, $\rho_{ti}$ is the thermal ion Larmor radius, and $L_{ti}$ is the ion temperature scale length. If one computes heat sources based on a power balance in such a situation, a Bohm like scaling means increasing power input with the plasma size, while a gyro-Bohm like scaling corresponds to constant power input regardless of the plasma size. Therefore, the size scaling studies based on $\delta f$ gyrokinetic simulations implicitly involve influences of the dependency of turbulent transport on heating power or the power scaling, which significantly affects global confinement scalings.[3] In addition, the gyro-Bohm like scaling may not be relevant for future large devices, in which total heating power including self-heating by the fusion-generated alpha particles will be significantly larger than auxiliary heating in the present experiments.

In this Letter, we revisit the plasma size scaling of ion heat transport induced by ITG turbulence using the full-$f$ gyrokinetic Eulerian code GT5D.[8] We perform a series of fixed-flux simulations where both plasma size and heating power are scaled and discuss influences of the power scaling on the transport scaling for large devices. In Ref. 9, the plasma size and power scaling of ITG turbulence was first investigated for small devices ($\rho^{*-1} = 100 \sim 225$), and the so-called worse-than-Bohm scaling of turbulent transport[1] and the gyro-Bohm like scaling of turbulent fluctuations[10] were simultaneously recovered using GT5D. However, in such small device parameters, plasma size effects are not well separated from influences of heating power. In this study, we extend the plasma size up to the local limit regime ($\rho^{*-1} > 300$), where the former effects become small enough, and investigate the latter effects.

We consider electrostatic ITG turbulence with gyrokinetic ions and adiabatic electrons in a circular concentric tokamak configuration with $R/a = 2.79$ and $q(r) = 0.85 + 2.18(r/a)^2$, which has Cyclone like parameters[11] at midradius $r_s = 0.5a$: $\epsilon = r_s/R \sim 0.18$, $q(r_s) \sim 1.4$, $\hat{s}(r_s) = [(r/q)dq/dr]_{r=r_s} \sim 0.78$, $n_e \sim 4.6 \times 10^{19}\mathrm{m}^{-3}$, $T_e \sim T_i \sim 2\mathrm{keV}$, $R/L_n = 2.22$. Here, $q$ is the safety factor, $\epsilon$ is the local inverse aspect ratio, $n_e$ is the density, $T_e$ and $T_i$ are the electron and ion temperature, and $L_n$ is the density scale length. The normalized collisionality is $\nu^* = \epsilon^{-3/2}\nu_{ii}qR/v_{ti} \sim 0.072$ at $r = r_s$, where $\nu_{ii}$ is the ion-ion collision frequency and $v_{ti}$ is the ion thermal velocity. Auxiliary heating is given by a source term, $S_{src} = \nu_h A_{src}(r)(f_{M1} - f_{M2})$, where $A_{src}(r)$ is a deposition profile of on-axis heating ($r/a = 0 \sim 0.4$). The heating rate $\nu_h$ and two Maxwellian distribution functions with different temperatures, $f_{M1}$, $f_{M2}$, are chosen to impose fixed power input $P_{in}$ with no momentum input. A L-mode like boundary condition with a fixed edge temperature $T_{i,r=a} = 0.8$ keV and no slip boundary is imposed by a Krook type sink operator $S_{snk} = \nu_s A_{snk}(r)(f - f_0)$, where $f$ is the ion guiding-center distribution function, $f_0$ is the initial

 

distribution function, $A_{snk}(r)$ is localized near the plasma surface ($r/a = 0.9 \sim 1$), and the sink parameter $\nu_s \sim 0.1 v_{ti}/a$ is chosen to fix the edge temperature and rotation. The initial ion temperature profile is set as $R/L_{ti} = 10$ at $r = r_s$, which is far above linear and nonlinear thresholds at $R/L_{ti} = 3 \sim 3.5$ and at $R/L_{ti} \sim 6$, respectively. This leads to strong excitation of linear ITG modes followed by initial transient bursts, which accelerate temperature relaxation processes towards steady states. Although full-$f$ simulations, in general, require confinement time scale simulations to compute steady plasma profiles and transport levels, the above linearly unstable initial condition enables us to obtain approximately converged quasi-steady states in a few collision times.[12] Therefore, we discuss transport levels and temperature profiles in quasi-steady states, typically, after $\sim 1000 R/v_{ti}$ ($\sim$10 ms for $\rho^{*-1} \sim 600$). The plasma size and heating power are chosen as $(\rho^{*-1}, P_{in}) = (150, 4\text{MW})$, (300,8 MW), (450,12 MW), and (600,16 MW). Here, $\rho^*$ is estimated by using the volume-averaged initial ion temperature. The corresponding $\rho^*$ values estimated by the steady ion temperature at $r/a = 0.5$ are $\rho^{*-1} = 130$, 259, 389, and 520, respectively. All the simulations are performed using a 1/6 wedge of the full torus, in which transport levels are converged with respect to wedge size.[9] Five dimensional grids for $f$ are scaled as $(N_R, N_\zeta, N_Z, N_{v\parallel}, N_{v\perp}) = (160, 32, 160, 96, 20) \sim (610, 128, 610, 96, 20)$ for $\rho^{*-1} = 150 \sim 600$, where a configuration space is discretized using the cylindrical coordinates $(R, \zeta, Z)$. The electrostatic potential $\phi$ is computed using finite elements with $(N_r, N_\theta, N_\zeta) = (128, 256, 32) \sim (512, 1024, 128)$ in the flux coordinates $(r, \theta, \zeta)$. Here, $\zeta$ and $\theta$ are the toroidal angle and the (straight-field-line) poloidal angle. Dirichlet boundary conditions are used for both $f$ and $\phi$ while an effective physical boundary condition of $f$ is imposed by the above sink term. In GT5D, a modern gyrokinetic theory[13] is implemented using a non-dissipative and conservative finite difference scheme,[14] which exactly conserve $f$ and its arbitrary moments. Ion-ion collisions are computed by a linear Fokker-Planck operator with a conservative field particle operator.[15] These conservative schemes enable robust long time turbulence simulations by conserving the particle number, the toroidal angular momentum, and the energy.[8,16]

The above plasma parameters give a Bohm like scaling or the normalized heat diffusivity $\chi_i/\chi_{GB}$ proportional to the plasma size, provided that $R/L_{ti}$ is unchanged. By using this condition, one can clearly test two extreme situations, increasing (Bohm like) $\chi_i/\chi_{GB}$ with constant $R/L_{ti}$ and constant (gyro-Bohm like) $\chi_i/\chi_{GB}$ with increasing $R/L_{ti}$, which are different from the situation of $\delta f$ simulations: constant $\chi_i/\chi_{GB}$ with constant $R/L_{ti}$ for $\rho^{*-1} > 300$. Figure 1 shows $\chi_i/\chi_{GB}$ and $R/L_{ti}$ observed in a series of numerical experiments. The ion temperature gradient falls down from the initial condition $R/L_{ti} = 10$ to the quasi-steady state $R/L_{ti} \sim 6$, which is limited by the nonlinear critical gradient. Because of the stiff ion temperature profiles, $\chi_i/\chi_{GB}$ increases with the plasma size following the power balance. Unlike former $\delta f$ simulations, the present numerical experiments show increasing $\chi_i/\chi_{GB}$ with the similar $R/L_{ti}$ even in the local limit regime. It is noted that the local flux-tube gyrokinetic

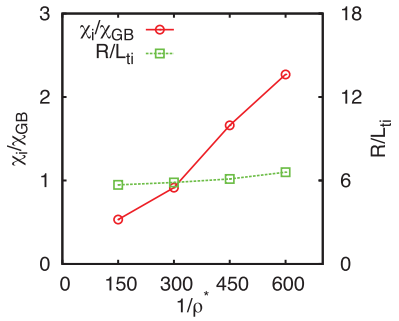


FIG. 1. The ion heat diffusivity $\chi_i/\chi_{GB}$ ($\chi_{GB} = \rho_{ti}^2 v_{ti}/L_n$) and the ion temperature gradient $R/L_{ti}$ observed at $r/a \sim 0.5$ in the ITG turbulence simulations with $(\rho^{*-1}, P_{in}) = (150, 4\text{MW})$, (300,8 MW), (450,12 MW), and (600,16 MW).

Eulerian code GKV[17] gives $\chi_i/\chi_{GB} \sim 2.5$ at $R/L_{ti} = 6$. Compared with this local limit value, present full-$f$ simulations tend to give lower transport levels in the local limit regime. In Ref. 18, it was confirmed that at $\rho^{*-1} = 450$, GT5D with a fixed-gradient source model recovers a local limit value estimated by GKV. Therefore, the difference in transport levels is attributed to a fixed-flux nature of the source model. This tendency was found also in the former benchmark study,[19] where full-$f$ simulations used significantly higher temperature gradients $R/L_{ti} \sim 10$ to reach at transport levels of $\delta f$ simulations with $R/L_{ti} \sim 7$.

In Ref. 18, transport properties of the $\rho^*$ scan were investigated in detail. Turbulent correlation length $\Delta r$ and correlation time $\Delta t$ show a gyro-Bohm like dependency with $\Delta r = 6 \sim 7\rho_{ti}$ and $\Delta t = 2 \sim 3 v_{ti}/a$. For large devices with $\rho^{*-1} > 300$, profile shearing due to the density, temperature, and mean radial electric field $E_r$ profiles decreases with the plasma size, and a dominant shearing effect comes from turbulence driven zonal flows $E_{ZF}$, which has meso-scale structures with similar scale lengths $\sim 20\rho_{ti}$ regardless of the plasma size. Heat fluxes show non-local transport due to radial propagation of avalanches and indicate self-organized critical phenomena such as $1/\omega$ frequency spectra. Low amplitude avalanches below the time-averaged transport level are typically trapped by a single zone of $E_{ZF}$, their propagation directions are determined by the sign of $E_{ZF}$ shear, and the propagation widths show a gyro-Bohm like dependency. On the other hand, large amplitude bursts propagate over significant radii across multiple zones of $E_{ZF}$. Such large scale avalanches carry about $\sim$70% of turbulent heat transport. Large scale avalanches are followed by quiescent phases, and transient drop and build-up of the temperature gradient are repeated following a local power balance. This process leads to higher super-critical states and larger amplitude bursts at smaller $\rho^*$ (and higher $P_{in}$), and gives different transport levels with the similar time-averaged temperature gradients. This transport property in the local limit regime can not be explained by the conventional plasma size effects such as profile shearing and turbulence spreading.

In order to understand the simulation result in Fig. 1, we focus on influences of the heating power on the transport scaling, and perform systematic power scans with fixed $\rho^*$. Plasma parameters are the same as the above $\rho^*$ scan except for the heat deposition profile ($r/a = 0 \sim 0.5$) and the collisionality ($\nu^* \sim 0.1$ at $r = r_s$). The above source term often produces

negative values of $f$, when high input power is localized in a small volume. To avoid such spurious phenomena at higher heating power, we use wider deposition profile and higher collisionality. This choice leads to slightly different transport levels (see $(\rho^{*-1}, P_{in}) = (150, 4\text{MW})$ cases in Fig. 4). In the power scan, long time ITG turbulence simulations are performed until the net (neoclassical and turbulent) heat flux matches the input power and the power balance is established. In the steady state, the core ion energy confinement time $\tau_{ion} = W_{ion}/P_{in}$ is computed from the core ion stored energy $W_{ion}$, in which a part of the ion stored energy sustained by the boundary temperature is subtracted. Figure 2 shows the power scaling of $\tau_{ion}$ for $\rho^{*-1} = 150$ and 225. In both scans, the degradation of confinement is observed with increasing heating power, and the power scalings are estimated as $\tau_{ion} \propto P_{in}^{-0.55}$ and $P_{in}^{-0.62}$, respectively. These results show the similar tendency as the power scaling of L-mode experiments, $\tau_E \sim P_{in}^{-0.73}$ (Ref. 3), and suggest the soundness of heating models and boundary conditions used in the present full-$f$ simulations, where $\tau_E$ is the energy confinement time.

In the power scan, turbulent correlation length and time are almost constant with $\Delta r = 5 \sim 6\rho_{ti}$ and $\Delta t = 2 \sim 3v_{ti}/a$, mean radial electric fields $E_r$ show the similar global structures, and zonal flows $E_{ZF}$ are also in the similar levels. However, as shown in Fig. 3, the frequency and amplitude of avalanche like heat fluxes are significantly increased with heating power. The core region is dominated by large scale avalanches, and the stiffness of ion temperature profiles is strong. On the other hand, in the outer region, small scale events appear at higher heating power, and ion temperature profiles become less stiff. The core stored energy is gradually increased with $P_{in}$ mainly due to changes in $R/L_{ti}$ in the outer region, while $R/L_{ti}$ at $r = r_s$ is almost constant. It is noted that when the same $P_{in}$ is imposed, $\tau_{ion}$ scales as gyro-Bohm like $\tau_{ion} \propto \rho^{*-3}$. However, because of less stiff temperature in the outer region, global ion temperature profiles are significantly different, and $\rho^{*-1} = 150$ cases give higher core temperature. If one chooses $P_{in}$, which gives the similar temperature profiles, as in the experiment,[1] the resulting $\rho^*$ scaling is (worse-than) Bohm like.[9]

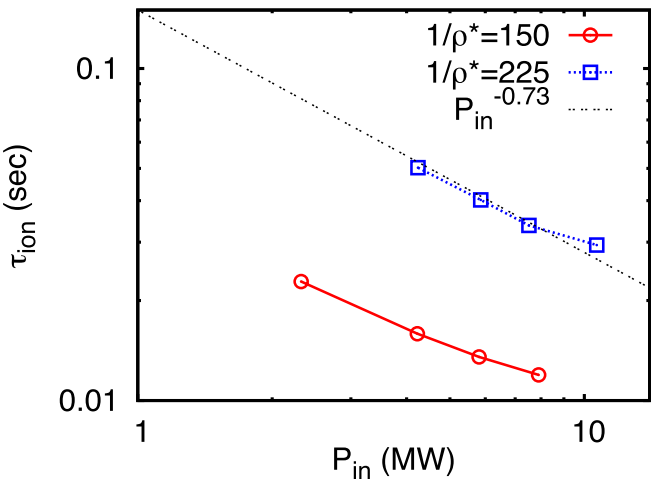


FIG. 2. The power scaling of the core ion energy confinement time $\tau_{ion}$ in ITG turbulence simulations with $\rho^{*-1} = 150$ and 225.

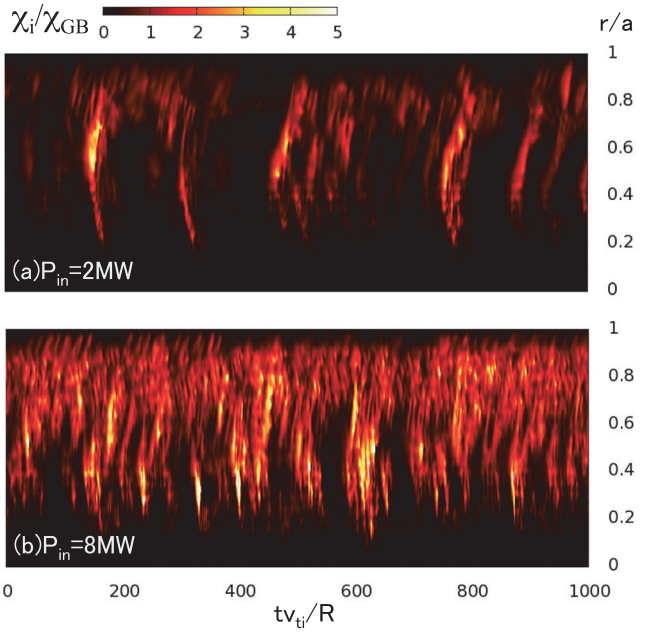


FIG. 3. The spatio-temporal evolutions of the normalized heat diffusivity $\chi_i/\chi_{GB}$ observed in the power scan with $(\rho^{*-1}, P_{in}) = (150, 2\text{MW}), (150, 8\text{ MW})$.

In Fig. 4, the stiffness of the ion temperature profile is compared between the $\rho^*$ (and $P_{in}$) scan and the power scan $(\rho^{*-1} = 150)$. In the power scan, it is clearly seen that a nonlinear critical gradient exists at $R/L_{ti} \sim 6$,[8,11] and the heat flux $q_i$ rapidly increases above the nonlinear critical gradient. This feature provides stiff ion temperature profiles leading to the power degradation of confinement. It is noted that in the lowest power case, neoclassical and turbulent heat fluxes are comparable, and such criticality does not appear. The $\rho^*$ scan also shows the similar stiffness, and $R/L_{ti}$ slowly increases with heating power. According to Fig. 4, enormous heating power is needed to achieve higher temperature gradients beyond the nonlinear critical gradient.

The similarity of transport properties between the $\rho^*$ scan and the power scan is also seen in the probability

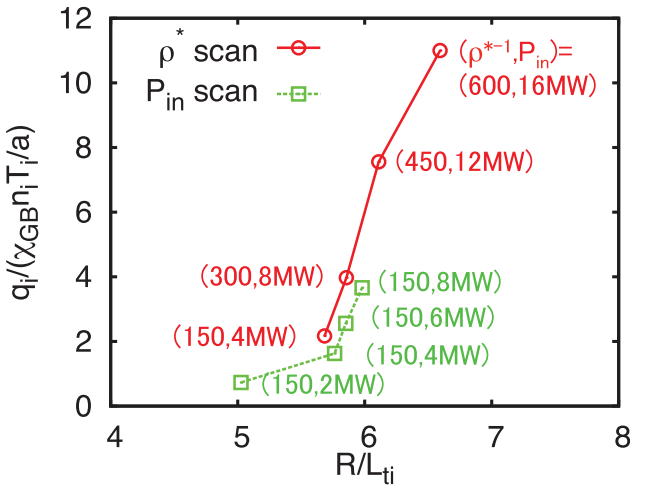


FIG. 4. Comparisons of the stiffness of the ion temperature profile between the $\rho^*$ (and $P_{in}$) scan and the power scan $(\rho^{*-1} = 150)$. The normalized turbulent heat flux $q_i/(\chi_{GB} n_i T_i/a)$ is plotted against the temperature gradient $R/L_{ti}$. The data are observed at $r/a \sim 0.5$.

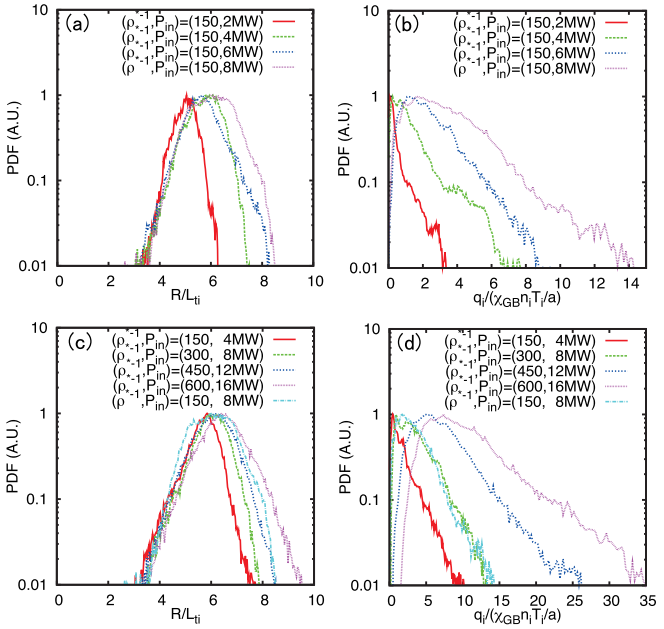


FIG. 5. The probability distribution functions of the normalized turbulent heat flux $q_i/(\chi_{GB} n_i T_i/a)$ (b), (d) and the ion temperature gradient $R/L_{ti}$ (a), (c) at $r/a = 0.5$. (a)–(d) show the $P_{in}$ $(\rho^*)$ scan. In (c) and (d), $(\rho^{*-1}, P_{in}) = (150, 8\text{MW})$ case is also included for comparison.

distribution functions (PDFs) of $R/L_{ti}$ and $q_i$ in Fig. 5. In the power scan, the PDFs of $R/L_{ti}$ become broader as heating power increases. They show the same lower limit, which is constrained by the linear critical gradient, while the higher limit is significantly extended with heating power. This leads to higher transient super-critical states with the similar time averaged temperature gradients, and the PDFs of $q_i$ shows significant extension of tail components reflecting larger amplitude bursts. The $\rho^*$ scan also shows the similar changes in the PDFs of $R/L_{ti}$ and $q_i$, and the PDFs of $q_i$ show large tail components at higher heating power. It is noted that in the $\rho^*$ scan, the linear critical gradient is varied from $R/L_{ti} \sim 3.5\,(\rho^{*-1} = 150)$ to $R/L_{ti} \sim 3\,(\rho^{*-1} = 600)$, and the above effect may be more pronounced. This kind of non-Gaussian feature is qualitatively different from a Gaussian feature observed in Ref. 5. Interestingly, in Fig. 5(d), the PDFs of $q_i$ with $(\rho^{*-1}, P_{in}) = (150, 8\text{MW})$ and (300,8 MW) show almost the same profile. These observations suggest that the transport scaling in the present $\rho^*$ scan is dominated by the power scaling of turbulent transport.

In summary, the present study clarified critical roles of the power scaling of turbulent transport in predicting the performance of future large devices. Through systematic power scans of ITG turbulence using fixed-flux full-$f$ simulations, the stiffness of ion temperature profile and the related power degradation of confinement are shown by first principles calculations. The PDFs of $R/L_{ti}$ and $q_i$ show significant extension of tail components at higher heating power, and transient super-critical states drive larger amplitude bursts. As a result, even with the similar time-averaged temperature gradients, significantly larger turbulent transport is induced depending on heating power. This kind of non-Gaussian feature induced by fluctuating temperature profiles is essential for reproducing the power scaling of turbulent transport.

Influences of the power scaling of turbulent transport were implicitly involved in former $\rho^*$ scaling studies based on fixed-gradient gyrokinetic simulations, which reported gyro-Bohm like scaling in the local $(\rho^* \to 0)$ limit regime. In contrast, in the present $\rho^*$ scaling study, heating power is explicitly scaled with plasma size, and it is found that the transport scaling is significantly affected by the power scaling of turbulent transport, and even in the local limit regime, the heat diffusivity may increase with plasma size depending on heating power.

The simulations were performed on the K-computer at the Riken, the Helios at the IFERC, and the BX900 at the JAEA. This work was supported by the MEXT, Grant for HPCI Strategic Program Field No. 4: Next-Generation Industrial Innovations and Grant No. 22866086.

[1]C. C. Petty, T. C. Luce, R. I. Pinsker, K. H. Burrell, S. C. Chiu, P. Gohil, R. A. James, and D. Wroblewski, Phys. Rev. Lett. **74**, 1763 (1995).
[2]H. Shirai, T. Takizuka, O. Naitou, M. Sato, N. Isei, Y. Koide, T. Hirayama, and M. Azumi, J. Phys. Soc. Jpn. **64**, 4209 (1995).
[3]ITER Physics Expert Groups on Confinement and Transport and Confinement Modelling and Database, ITER Physics Basis Editors, and ITER EDA, Nucl. Fusion **39**, 2175 (1999).
[4]X. Garbet, Y. Idomura, L. Villard, and T. H. Watanabe, Nucl. Fusion **50**, 043002 (2010).
[5]Z. Lin, S. Ethier, T. S. Hahm, and W. M. Tang, Phys. Rev. Lett. **88**, 195004 (2002).
[6]T. S. Hahm, P. H. Diamond, Z. Lin, K. Itoh, and S.-I. Itoh, Plasma Phys. Control. Fusion **46**, A323 (2004).
[7]B. F. McMillan, X. Lapillonne, S. Brunner, L. Villard, S. Jolliet, A. Bottino, T. Gorler, and F. Jenko, Phys. Rev. Lett. **105**, 155001 (2010).
[8]Y. Idomura, H. Urano, N. Aiba, and S. Tokuda, Nucl. Fusion **49**, 065029 (2009).
[9]S. Jolliet and Y. Idomura, Nucl. Fusion **52**, 023026 (2012).
[10]G. R. McKee, C. C. Petty, R. E. Waltz, C. Fenzi, R. J. Fonck, J. E. Kinsey, T. C. Luce, K. H. Burrell, D. R. Baker, E. J. Doyle, X. Garbet, R. A. Moyer, C. L. Rettig, T. L. Rhodes, D. W. Ross, G. M. Staebler, R. Sydora, and M. R. Wade, Nucl. Fusion **41**, 1235 (2001).
[11]A. M. Dimits, G. Bateman, M. A. Beer, B. I. Cohen, W. Dorland, G. W. Hammett, C. Kim, J. E. Kinsey, M. Kotschenreuther, A. H. Kritz, L. L. Lao, J. Mandrekas, W. M. Nevins, S. E. Parker, A. J. Redd, D. E. Shumaker, R. Sydora, and J. Weiland, Phys. Plasmas **7**, 969 (2000).
[12]Y. Idomura, "Full-f gyrokinetic simulation over a confinement time," Phys. Plasmas. (to be published).
[13]A. J. Brizard and T. S. Hahm, Rev. Mod. Phys. **79**, 421 (2007).
[14]Y. Idomura, M. Ida, T. Kano, and S. Tokuda, Comput. Phys. Commun. **179**, 391 (2008).
[15]S. Satake, Y. Idomura, H. Sugama, and T.-H. Watanabe, Comput. Phys. Commun. **181**, 1069 (2010).
[16]Y. Idomura, Comput. Sci. Disc. **5**, 014018 (2012).
[17]T.-H. Watanabe and H. Sugama, Nucl. Fusion **46**, 24 (2006).
[18]M. Nakata and Y. Idomura, Nucl. Fusion **53**, 113039 (2013).
[19]Y. Sarazin, V. Grandgirard, J. Abiteboul, S. Allfrey, X. Garbet, Ph. Ghendrih, G. Latu, A. Strugarek, G. Dif-Pradalier, P. H. Diamond, S. Ku, C. S. Chang, B. F. McMillan, T. M. Tran, L. Villard, S. Jolliet, A. Bottino, and P. Angelino, Nucl. Fusion **51**, 103023 (2011).